ELSEVIER

Journal of Power Sources 86 (2000) 449–454

JOURNAL OF POWER SOURCES

www.elsevier.com/locate/jpowsour

The influence of the mass transfer on the geometric design of SOFC stacks

Wolfgang Winkler *

FSP Brennstoffzellen und rationelle Energieversorgung, University of Applied Sciences-Fachhochschule Hamburg, Berliner Tor 21, D 20099 Hamburg, Germany

Accepted 26 October 1999

Abstract

The system cost of any SOFC plant and the chances of development of a mobile SOFC application strongly depend on the power density of the stack. Good mass transfer within the stack is one important physical requirement for high power density. The influences on the mass transfer in a tubular, a tubular–annular and a planar stack are analyzed and discussed. It results in a proposal for a tubular–helix SOFC stack to increase the mass transfer by better mixing.

Keywords: SOFC; Mass transfer; Power density

1. Introduction

The power density of a SOFC stack influences the size of the insulation and of the containment — e.g., a pressure vessel for a SOFC-GT — and thus, the system cost. Therefore, high power density is important to reduce the system cost. It is essential for any mobile application of a power system to require as little space as possible and to leave the available space for the pay load. Thus, the design task achieved again a high power density. It is clear that an optimised geometry of a stack delivers a maximum possible active surface area per unit volume. The mass transfer within the fuel channels and within the air channels of the stack must assure mass flow of the reactant gas and the product gas to and from the electrodes. However, it is still necessary to obtain experimental results, although an analytical approach beforehand helps to define the problems more clearly and to show principal solutions. Fig. 1 shows the definition of the problem.

The tubular design has some geometric and operational benefits compared with a planar design as already shown in a design analysis [1,2]. Small tube diameters allow an excellent start up performance and deliver a very high power density [3,4]. The main aim here is to analyse the influence of the stack geometry on mass transfer within the stack and to suggest measures that can be adopted to increase the mass transfer.

2. Mass transfer and SOFC stack geometry

The molar transfer flux, $'N_X$, (mol/s) between a wall and the bulk flow is defined by:

$$'N_X = \beta A \Delta c_X, \quad (1)$$

β is the mass transfer coefficient (m/s), A is the active area (m^2) and Δc_X (mol/m^3) is the concentration gradient between the bulk flow and the solid surface. The mass transfer coefficient can be calculated as for the heat transfer coefficient if we use the Sherwood number, Sh, and the Schmidt number, Sc, instead of the Nusselt number, Nu, and the Prandtl number, Pr, in the expressions of an appropriate heat transfer expression. The Sherwood number, Sh, is defined as:

$$\mathrm{Sh} = \beta (L/D), \quad (2)$$

L is the characteristic length (m) and D is the diffusion coefficient (m^2/s). The Schmidt number, Sc, is defined as:

$$\mathrm{Sc} = \nu / D, \quad (3)$$

* Tel.: +49-42-859-3137; fax: +49-40-428-59-2658; e-mail: winkler@rzbt.fh-hamburg.de

PII: S0378-7753(99)00452-8

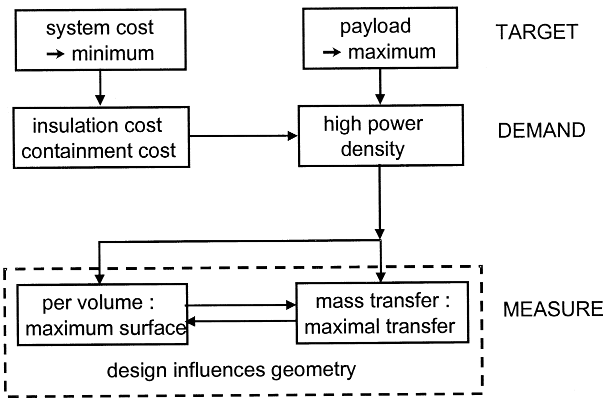

Fig. 1. Design targets of SOFC stacks and the influence on the mass transfer.

ν is the kinematic viscosity. The third dimensionless number — the Reynolds number, Re — is defined with the velocity, w (m/s) as:

$$Re = w(L/\nu). \tag{4}$$

Within Eq. (4), the hydraulic diameter, d_H, of the flow channel considered the characteristic length, L, for all types of stacks is incorporated. The length of the flow channel is le and the Sherwood number, Sh, can be calculated from expressions of the form.

$$\mathrm{Sh} = \mathrm{Sh}(Re, d_H/\mathrm{le}, \mathrm{Sc}). \tag{5}$$

The expressions to be used for the different problems can be derived from appropriate heat transfer equations, for example, in Ref. [5]. The influence of the stack geometry on mass transfer within the stack is obtained by using Eqs. (1)–(5), in Fig. 2.

It can be seen immediately, that a decreasing hydraulic diameter, d_H, leads to an increasing mass transfer coefficient, β. The Reynolds number, Re, and the ratio d_H/le of the hydraulic diameter and the channel length are the other important geometric influences on the Sherwood number, Sh, and, thus, on the mass transfer. The velocity, w, depends on the mass flow, $'m$, itself dependent on the fuel cell process and on the area, A_q, of the free cross-section of the flow channel. These influences on the Reynolds number, Re, can be expressed by an appropriate expression of w. The flow velocity, w, is defined as:

$$w = 'm/(A_q \rho), \tag{6}$$

$'m$ is the mass flow of the fluid and ρ is the density of the fluid. The mass flow of the fuel, $'m_F$, and the mass flow of the air, $'m_A$, are related by:

$$'m_A = \lambda \mu_{A0} {'m_F}, \tag{7}$$

if it is assumed that all the total fuel is used in the cell system. The excess air is λ and the fuel related stoichiometric air demand is μ_{A0}. The fuel utilised within the SOFC stack is:

$$'m_{FU} = 'm_F U_F; \tag{8}$$

U_F is the fuel utilisation. The fuel, $'m_{FU}$, utilised yields an electrical current, I:

$$'m_{FU} = M_F I/(n_{el} F), \tag{9}$$

n_{el} is the number of electrons per fuel molecule utilised. M_F is the molar mass of the fuel and F is the Faraday constant. The Reynolds number of the fuel flow, F, and of the air flow, A, can be written as:

$$Re_F = M_F/(\rho_F n_{el} F \nu_F U_F) I d_{HF}/A_{qF} \tag{10}$$

and

$$Re_A = \lambda \mu_{A0} M_F/(\rho_A n_{el} F \nu_A U_F) I d_{HA}/A_{qA}. \tag{11}$$

If the current density is i (A/m^2) and the active area is A_a then:

$$I = iA_a \tag{12}$$

and the hydraulic diameter, d_H, is given by:

$$d_H = 4A_q/\mathrm{Pe}. \tag{13}$$

Pe is the wetted perimeter. Then, Eqs. (10)–(13) yield:

$$Re_F = 4M_F/(\rho_F n_{el} F \nu_F U_F) iA_a/\mathrm{Pe}_F \tag{14}$$

for the fuel channel and:

$$Re_A = 4\lambda \mu_{A0} M_F/(\rho_A n_{el} F \nu_A U_F) iA_a/\mathrm{Pe}_A. \tag{15}$$

for the air channel.

Eqs. (14) and (15) show that the characteristic length, L, is the ratio of the active area, A_a, and the wetted perimeter, Pe, if the influences of the stack during operation are included. We see that the Reynolds numbers in a fuel cell stack consists of three part, that can only be partially influenced by design and operation. These influences, and the consequences for stack design, will be discussed with respect to an example for the air channel. The influences in a fuel channel are similar. The influences on the Reynolds number, Re_A, can be expressed by three terms. The first term, ST_A, represents the influence of the substances and the thermodynamic state:

$$\mathrm{ST}_A = \mu_{A0} M_F/(\rho_A n_{el} F \nu_A), \tag{16}$$

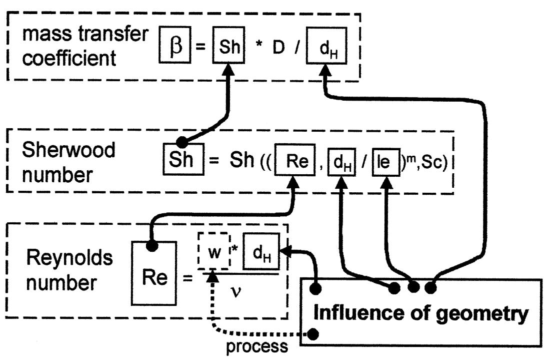

Fig. 2. The influence of the stack geometry on the mass transfer within the stack.

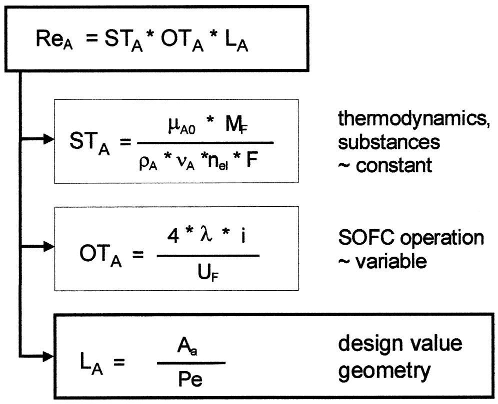

Fig. 3. The influences on the Reynolds number.

the second term, OT_A, represents the operating conditions of the cell:

$$OT_A = 4\lambda i / U_F \tag{17}$$

and the characteristic length, L_A, as the third term, represents the geometric influence:

$$L_A = A_a / Pe_A. \tag{18}$$

The Reynolds number can now be written:

$$Re_A = ST_A OT_A L_A = ST_A OT_A (A_a / Pe_A). \tag{19}$$

Fig. 3 shows the influences on the Reynolds number, Re_A, of the three terms listed above. ST_A represents the fuel used and the thermodynamic state mainly consists of physical constants. Only the dynamic viscosity $(\rho\nu)$ depends on the thermodynamic state being defined by the design of the fuel cell system. The term OT_A represents the operating conditions and can be changed by changes in the excess air, λ, the current density, I, and the fuel utilisation, U_F. These values can be varied in any test rig. An increase of the Reynolds number, Re_A, increases the dynamic effects, reduces the viscosity effects in the flow and changes the flow from laminar to turbulent at $Re_A = 2300$. The mass transfer increases with an increasing mixing of the flow. The mass transfer, thus, can be influenced by changing the parameters influencing the Reynolds number, Re_A. It is important to compare the values of the excess air, λ, the current density, i, and the fuel utilisation, U_F, with the design values of future commercial application by considering the experimental results, for example, of cells with a very high power density. The definition of the characteristic length, L, suggests a recommendation for the geometric design of stacks through an increase in the ratio of the active area, A_a, and the wetted perimeter, Pe, leading to an increase in the Reynolds number, Re_A, within the stack.

3. Usual SOFC stack geometry and the proposed tubular–helix design

It is necessary to apply the above equations in the configurations used for SOFC stacks. Fig. 4 shows the configurations considered: a tubular SOFC, a tubular SOFC with an annular channel, called here tubular–annular SOFC, and a planar SOFC with a rectangular channel.

The active area, A_{aT}, of the tubular SOFC is:

$$A_{aT} = d\pi \,\mathrm{le}, \tag{20}$$

with a tube diameter, d, and the length, le, of the tube. Eq. (20) includes the tubular–annular SOFC. It is assumed that the electrodes and the electrolyte are thin compared with the diameter, d. This gives, for the tubular SOFC by using Eqs. (13), (18) and (20) and Fig. 4:

$$L_T = \mathrm{le}, \tag{21}$$

$$d_{HT} = d \tag{22}$$

and for the tubular–annular SOFC:

$$L_{TA} = \mathrm{le}\, d / (d + d_i) \tag{23}$$

$$d_{HTA} = d - d_i. \tag{24}$$

For the planar SOFC:

$$A_{aT} = 2b\,\mathrm{le}, \tag{25}$$

$$L_P = \mathrm{le}\, b / (b + h) \tag{26}$$

and

$$d_{HP} = 2bh / (b + h), \tag{27}$$

if the electrode covered with the contact fin is included in the total active area. The benefits of the tubular–annular SOFC and the planar SOFC are, that the hydraulic diameter, d_H, can be influenced by the design of the channels by varying the height, h, of the channel.

The design aim is to increase the characteristic length, L, and to decrease the hydraulic diameter, d_H, whilst increasing the Reynolds number as little as possible. As mentioned above, an increase in the mixing within the flow channels increases the mass transfer. The best mixing can be obtained in a turbulent flow, with $Re > 2300$. The product, $ST_A OT_A$, usually an the order of magnitude $\sim 10^2$. Thus, the length, le, of the channel must have an order of magnitude $> 10^1$ to reach a turbulent flow. A channel

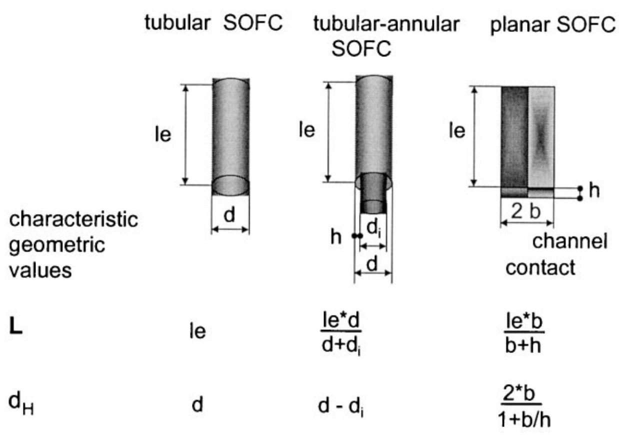

Fig. 4. Geometry, characteristic length L and hydraulic diameters d_H of different SOFC stack designs.

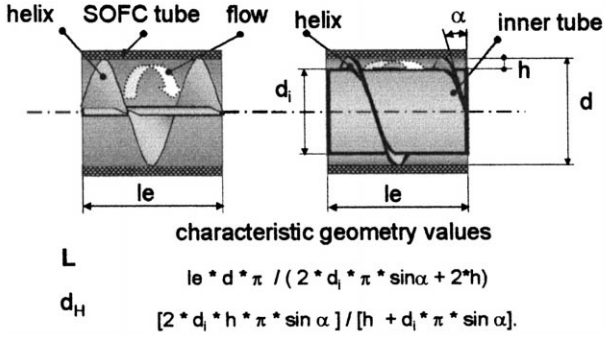

Fig. 5. The proposed tubular–helix SOFC design.

length of more than 10 m is not easy to attain with the designs of Fig. 4. The other possibility for increasing the mass transfer is to decrease the hydraulic diameter, d_H, to increase the mass transfer coefficient, β, as defined in Eq. (2).

The length of the flow channel within a tubular SOFC can be clearly increased if a helix is placed within the tube. Fig. 5 shows the proposed tubular–helix design and the characteristic geometric values. The helix can be placed in the tubular and in the tubular–annular SOFC as well.

In the latter case, the inner tube can be used to support the helix. A comparable helix can be used to design the contacts and channels on the outer, fuel side of the SOFC tube.

This proposed design has the following benefits:

- the length of the flow channel can be increased compared with the tube's length,
- the cross-section of the flow channel can be varied and
- the secondary flow due to the rotation of the flow increases mixing.

Using Fig. 5 and Eq. (18), we get for the characteristic length, L_{TX}, and the hydraulic diameter, d_{HTX}, of the tubular–helix design are given by:

$$L_{TX} = \text{le}\, d\pi/(2 d_i \pi \sin\alpha + 2h). \tag{28}$$

and

$$d_{HTX} = 2h(d - 2h)\pi\sin\alpha/[h + (d - 2h)\pi\sin\alpha] \tag{29}$$

with

$$h = (d - d_i)/2. \tag{30}$$

A rectangular cross-section was assumed in the above equations as a simplification of the segments of an ellipse, defining an intersection between helix and tubes.

It is necessary to verify these calculations by experiments and to confirm this application for fuel cells. Interesting results can be obtained by the following theoretical calculations to estimate the influences. The calculations are performed for a laminar flow.

For the tubular and the planar SOFC, by using the equations for the description of the mass transfer within a SOFC, the following are obtained:

$$\text{Sh}_{l/P,T} = \left[3.66^3 + 1.61^3(\text{Sc}\, Re\, d_H/\text{le})\right]^{1/3}. \tag{31}$$

And for the laminar flow, l, in a tubular–annular SOFC:

$$\text{Sh}_{l/TA} = \left\{\text{Sh} + \text{fd}\, 0.19(Re\,\text{Sc}\, d_{HTA}/\text{le})^{0.8} \Big/ \left[1 + 0.117\,(Re\,\text{Sc}\, d_{HTA}/\text{le})^{0.467}\right]\right\} \times (\text{Sc}/\text{Sc}_W)^{0.11}. \tag{32}$$

with

$$\text{Sh} = 3.66 + 1.2(d_i/d)^{0.5} \tag{33}$$

and

$$\text{fd} = 1 + 0.14(d_i/d)^{1/3}. \tag{34}$$

The index, W, in Eq. (32) stands for ''wall''.

The proposed tubular–helix design can be roughly described by the equations of Schmidt for tubular–helix heat exchangers as published in Ref. [5] chapter Gc. The original values have a deviation of ±15%. For the laminar flow inside a tubular helix SOFC:

$$\text{Sh}_{l/TX} = \left\{3.66 + 0.08\left[1 + 0.8(d_{HTX}/D)^{0.9}\right] \times Re^m\, \text{Sc}^{1/3}\right\}(\text{Sc}/\text{Sc}_W)^{0.14} \tag{35}$$

with:

$$m = 0.5 + 0.2903(d_{HTX}/D)^{0.194}. \tag{36}$$

D is the mean diameter of the helix. The critical Reynolds number, Re_{crit}, is defined as:

$$Re_{crit} = 2300\left[1 + 8.6(d_{HTX}/D)^{0.45}\right]. \tag{37}$$

4. Comparison of the different SOFC stack designs

The Eqs. (1)–(37) allow an estimation of the mass transfer coefficient, β, in the different types of SOFC

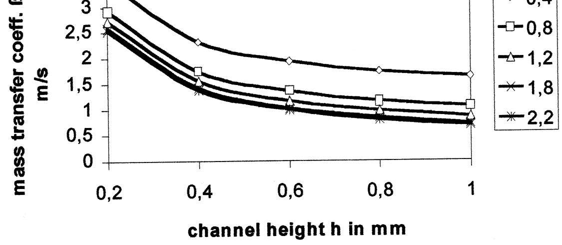

Fig. 6. The mass transfer coefficient, β, in a planar SOFC.

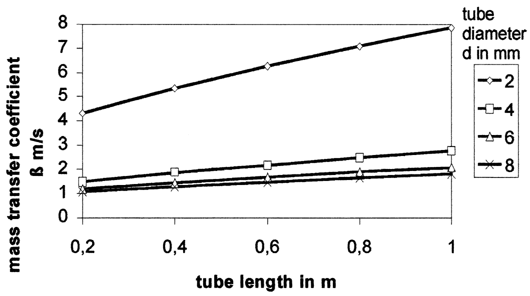

Fig. 7. The mass transfer coefficient in a tubular–helix SOFC.

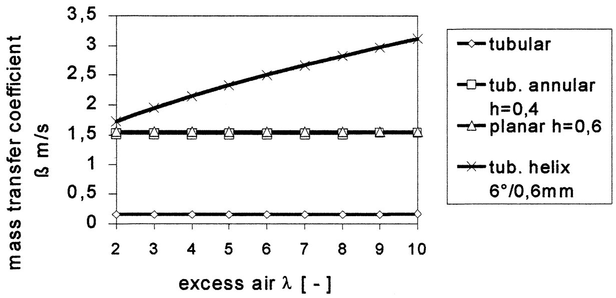

Fig. 8. The mass transfer coefficient in different SOFC stack designs depending on the excess air.

stacks. The analysis showed that the most restrictions occur on the inner side of a tubular design. It was assumed that this is the cathode side. The following considerations will be applied to the air channels of the SOFC therefore. The temperature is 1000°C, the excess air is 2, the fuel utilisation is 0.9 and the current density is 200 mA/cm^2 for all calculations; the SOFC length, le, is 1 m, if not specifically mentioned. It is interesting to note, that the channel length, le, influences only the Reynolds number, *Re*, and not the Sherwood number, Sh, of a planar SOFC, a tubular SOFC and a tubular–annular SOFC, because $Sh_{l/P,T}$ Eq. (31) and $Sh_{l/TA}$ Eq. (32) depend on Re_A d_H/le and le disappears for a linear correlation between *Re* and le.

The results of the calculations for a planar SOFC are shown in Fig. 6 as a function of the channel height, *h*, with the channel width, *b*, as a parameter. The mass transfer coefficient, β, increases with a decreasing channel height, *h*, and a decreasing channel width, *b*. A channel width $b > 1.8$ mm and a channel height, $h > 1$ mm does not really influence the mass transfer coefficient, β. The range of interest for the channel width, *b*, and the channel height, *h*, at which the mass transfer increases is close to the values of the thickness of the SOFC itself. Small values of the channel width, *b*, and the channel height, *h*, lead to high values of the mass transfer coefficient, β, as expected by Eq. (2).

The results of the calculations for a tubular–helix SOFC are shown in Fig. 7 as a function of the tube length, le, with the tube diameter, *d*, as a variable parameter. The mass transfer coefficient, β, increases with an increasing tube length, le, and a decreasing tube diameter, *d*. The tube diameter, *d*, influences the mass transfer coefficient, β, if the diameter, *d*, is about 2 mm.

Fig. 8 shows the influence of the excess air, λ, on the mass transfer coefficient, β, within the different designs. The influence of the excess air, λ, is for all linear flow channels (tubular, tubular–annular and planar) small because the products Re_A d_H/le are small. Only the tubular–helix design is independent on the product Re_A d_H/le and shows a clear increase of the mass transfer coefficient, β, by increasing the excess air, λ. This is an indication of the influence of the mixing effects by the helix geometry.

Fig. 9 shows a comparison of the different stack types as a function of the tube diameter or the channel width, *b*, for the planar design, respectively. A decreasing value of these figures leads to an increasing mass transfer coefficient, β, for all designs as expected by Eq. (2). But the tubular–annular design is an exception. The reason is that the relative value of a constant channel height, $h = (d - d_i)/2$ which increases with decreasing diameter, *d*, eventually leads to a tubular design with a disappearing inner diameter, d_i. It can be seen that the tubular–helix design

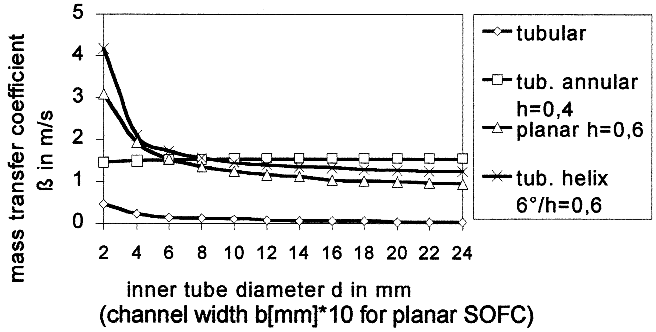

Fig. 9. The mass transfer coefficient in different SOFC stack designs depending on the channel geometry.

yields the highest values of the mass transfer coefficient for the designs compared in the area of interest having small diameters with a high power density.

5. Conclusions

The calculations show that a tubular–helix design of a SOFC stack can yield high mass transfer coefficients in a very small volume. These high values can be achieved with a short tube length for small tube diameters. The equations for calculating the Nusselt numbers of tubular–helix heat exchangers have been used to calculate the Sherwood number of a tubular–helix SOFC. This remains to be verified by actual experiments. The benefits of better mixing by this design and the clearly increased power density of small SOFC tubes is evident. Thus, further evaluation seems to be called for.

Acknowledgements

This work was carried out within the project: ‘‘Einsatz von Hochtemperaturbrennstoffzellen (SOFC) in der Energietechnik’’ (aFuE-FKZ 1701998) funded by the German Bundesministerium für Bildung und Forschung (BMBF). The author wishes to thank them for this funding.

References

[1] W. Winkler, European Fuel Cell News 5 (2) (1998) 9–14.
[2] W. Winkler, J. Krüger, Journal of Power Sources 71 (1998) 244–248.
[3] W. Winkler, J. Krüger, M. Sax, R. Telle, in: Philippe Stevens (Ed.), Proceedings 3rd European Solid Oxide Fuel Cell Forum in Nantes, Posters, 1998, pp. 245–254.
[4] T. Alston, K. Kendall, M. Palin, M. Prica, P. Windibank, Journal of Power Sources 71 (271) (1998) 271–274.
[5] VDI Wärmeatlas, 5, Aufl. VDI Verlag Düsseldorf, 1988.